Machine-Learning Downscaling of GRACE/GRACE-FO for Basin-Scale Groundwater Storage Assessment in a Semi-Arid Basin

Abba Ibrahim *, Aimrun Wayayok *, Helmi Zulhaidi Bin Mohd Shafri, Noorellimia Mat Toridi

Posted Date: 16 March 2026

doi: 10.20944/preprints202603.1157.v1

Keywords: terrestrial water storage; groundwater storage anomalies; spatial disaggregation; Random Forest; scale-dependent uncertainty; basin-scale groundwater assessment; semi-arid regions; remote sensing hydrology

 doi:10.20944/preprints202603.1157.v1

Article

Machine-Learning Downscaling of GRACE/GRACE-FO for Basin-Scale Groundwater Storage Assessment in a Semi-Arid Basin

Abba Ibrahim [1,2,*], Aimrun Wayayok [1,3,4,*], Helmi Zulhaidi Mohd Shafri [5] and Noorellimia Mat Toridi [1]

[1] Department of Biological and Agricultural Engineering, Faculty of Engineering, Universiti Putra Malaysia. 43400 UPM Serdang, Selangor DE, Malaysia

[2] Department of Agricultural and Environmental Engineering, Faculty of Engineering, Bayero University, Kano, Nigeria

[3] SMART Farming Technology Research Center (SFTRC), Faculty of Engineering, Universiti Putra Malaysia, 43400 UPM Serdang, Selangor DE, Malaysia

[4] International Institute of Aquaculture and Aquatic Sciences (I-AQUAS), Universiti Putra Malaysia, Mile 7, Kemang Rd. 6. Kemang Bay, Si Rusa, Port Dickson, Negeri Sembilan 71050, Malaysia.

[5] Department of Civil Engineering, Faculty of Engineering, Universiti Putra Malaysia. 43400 UPM Serdang, Selangor DE, Malaysia

* Correspondence: aibrahim.age@buk.edu.ng (A.I.), aimrun@upm.edu.my (A.W.)

Highlights

What are the main findings?

Random Forest downscaling reconstructs GRACE TWSA with high accuracy ($R^2 = 0.937$; NSE = 0.937) and preserves the original GRACE mass signal after redistribution to 1 km resolution.

- The downscaled product shows agreement with in-situ groundwater observations.

What are the implications of the main findings?

Kilometre-scale downscaling reveals sub-mascon groundwater heterogeneity that is not detectable in ~300 km GRACE products.

- The framework provides a transferable approach for enhancing GRACE-based groundwater monitoring when direct observations are limited.

Abstract

The Gravity Recovery and Climate Experiment (GRACE/GRACE-FO) missions provide terrestrial water storage anomalies (TWSA) at coarse spatial resolution (300km), limiting their application in medium-sized basins. This study develops a machine-learning framework to enhance the spatial interpretability of GRACE mascon TWSA within the 48,000 km² Hadejia-Jama'are River Basin, Nigeria. Hydroclimatic predictors derived from TerraClimate, Global Land Data Assimilation System (GLDAS), and Climate Hazards Group InfraRed Precipitation with Stations (CHIRPS) were integrated within a unified 4 km spatial framework. Four machine learning models were evaluated, including Random Forest (RF), Gradient Boosting, Histogram Gradient Boosting, and a Multi-Layer Perceptron. The RF model achieved the highest skill in reproducing mascon-scale TWSA ($R^2 = 0.937$; NSE = 0.937; RMSE = 4.36 cm). Aggregation of the 4 km fields back to the mascon scale preserved basin-integrated mass ($R^2 = 0.94$), confirming consistency with the original GRACE signal. The resulting groundwater storage anomaly (GWSA) fields resolve sub-basin spatial gradients and seasonal recharge-depletion cycles that are not discernible in the native product. Validation against 31 monitoring wells yielded moderate temporal agreement (Pearson correlation coefficient, r = 0.656), with magnitude discrepancies attributable primarily to scale mismatch and hydrogeological heterogeneity. While not a substitute for in-situ monitoring, the downscaled product enhances basin-

 doi:10.20944/preprints202603.1157.v1

scale groundwater assessment in data-scarce semi-arid regions. The framework is transferable to comparable basins and supports regional drought monitoring and water-resource management.

Keywords: terrestrial water storage; groundwater storage anomalies; spatial disaggregation; Random Forest; scale-dependent uncertainty; basin-scale groundwater assessment; semi-arid regions; remote sensing hydrology

1. Introduction

Groundwater monitoring is critical in semi-arid regions where abstraction pressures and climate variability intensify water-resource stress [1]. The Gravity Recovery and Climate Experiment (GRACE) and its successor GRACE-FO provide monthly terrestrial water storage anomaly (TWSA) estimates that integrate changes in groundwater, soil moisture, and surface water over large spatial footprints, and have been widely used to quantify large-scale groundwater depletion [2–4].

However, the coarse native spatial resolution of GRACE mascon and spherical-harmonic products (typical footprint scales of order of 10^5-10^6 km^2) limits direct application to small and many medium-sized basins, where sub-basin heterogeneity in recharge, abstraction, and hydrogeology plays an important role [2].

To increase the spatial utility of GRACE, researchers have developed downscaling methods that link coarse TWSA to finer-scale predictors [4]. Two broad approaches predominate: (i) dynamic assimilation and model-based downscaling, which embed GRACE within physically based hydrological or land-surface models [5–7] and (ii) statistical (empirical) downscaling, which uses data-driven relationships between GRACE TWSA and high-resolution predictor fields [8,9].

Over the past decade, machine-learning (ML) algorithms, including Random Forest (RF), Gradient-Boosting (GBR) and neural networks (NN), have become widely used for statistical downscaling because of their ability to capture nonlinear predictor-response relationships and complex interactions among hydroclimatic variables.

Recent studies demonstrate the feasibility of ML-based GRACE downscaling across diverse climates and hydrogeological settings. For example, Wang et al.[8] developed a 1-km GRACE-based groundwater storage product using a back-propagation neural network and accounted for time-lagged predictor effects, and reported strong correlation with ground observations in an arid region of China. Pulla et al. [9] proposed a flexible GRACE downscaler framework that supports multiple ML algorithms and produces 1-km fields, emphasizing model comparability and reproducibility. Li et al. [10] introduced a physically informed scaling-factor correction to reduce aggregation errors in downscaled GRACE products, improving mass conservation and local consistency. Other recent contributions include comparative evaluations of ensemble and hybrid ML models as well as multi-stage downscaling workflows that highlight both the potential for increased spatial detail and the persistence of scale-related uncertainties in GRACE-based groundwater estimates[11–28].

Despite these advances, important gaps remain and many ML downscaling approaches remain region-specific, with limited evidence regarding their transferability across hydroclimatic settings. Empirical disaggregation can also amplify uncertainty when predictor quality is limited or when groundwater systems exhibit delayed responses to climatic forcing. Furthermore, systematic validation against independent in-situ groundwater observations remains relatively scarce, particularly in data-scarce regions such as West Africa. In particular, the Hadejia-Jama'are River Basin (approximately 48,000 km^2) in northern Nigeria lacks published high-resolution GRACE-based groundwater assessments despite its semi-arid climate and strong dependence on groundwater resources.

This study develops and evaluates a ML-based framework to downscale terrestrial water storage anomalies derived from the Gravity Recovery and Climate Experiment for the Hadejia-Jama'are Basin. The framework integrates GRACE observations with globally available hydroclimatic predictors derived from satellite and reanalysis datasets, including precipitation estimates from the

 doi:10.20944/preprints202603.1157.v1

Climate Hazards Group InfraRed Precipitation with Stations (CHIRPS) dataset and climatic water balance variables from TerraClimate. By combining satellite gravimetry with machine-learning–based statistical inference, the approach generates kilometre-scale groundwater storage anomaly fields while maintaining consistency with basin-scale GRACE signals.

The primary objective of this study is to assess the capability of ML-based statistical downscaling to produce spatially refined groundwater storage anomalies in a semi-arid basin where hydrogeological observations are limited. Particular emphasis is placed on evaluating the consistency of the downscaled product with GRACE observations and its agreement with available groundwater monitoring data. By demonstrating the feasibility of GRACE downscaling in a semi-arid, data-limited basin, this work provides one of the first GRACE-based groundwater assessments for the Hadejia-Jama'are Basin and contributes to improving satellite-based groundwater monitoring in regions where conventional observations remain sparse.

2. Materials and Methods

2.1. Study Area

The study was conducted in the Hadejia-Jama'are River Basin (HJRB), a semi-arid basin in northern Nigeria covering approximately 48,000 km² (Figure 1). The basin lies between approximately 11°30′-13°30′ N latitude and 8°30′-11°30′ E longitude and forms part of the larger Komadugu-Yobe River system that ultimately drains into Lake Chad. The HJRB is hydrologically significant because it supports extensive agricultural activities, rural settlements, and ecologically important wetlands in an otherwise water-limited Sahelian environment [29,30].

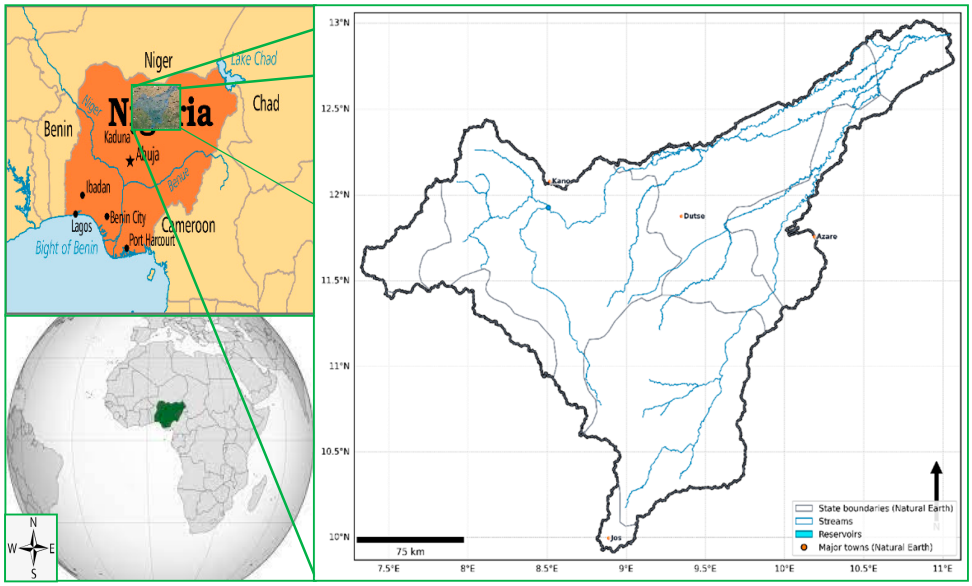

Figure 1. Study area location.

Climatically, the basin lies within the Sudan-Sahel climatic zone, characterized by strong seasonal rainfall variability associated with the northward and southward migration of the Intertropical Convergence Zone (ITCZ). The region experiences a distinct wet season from May to October, driven by moist southwesterly monsoon winds from the Atlantic Ocean, and a prolonged dry season from November to April, dominated by dry northeasterly Harmattan winds originating from the Sahara Desert [31].

Mean annual rainfall across the basin generally ranges between approximately 600 and 1000 mm, decreasing from the southern to the northern portions of the basin . Rainfall is highly variable

 doi:10.20944/preprints202603.1157.v1

both spatially and temporally and is largely controlled by the seasonal north–south movement of the Intertropical Discontinuity (ITD), which governs the onset and cessation of the West African monsoon in northern Nigeria [32]. Potential evapotranspiration in the basin is high and typically exceeds precipitation during most months of the year due to high temperatures, strong solar radiation, and low relative humidity. As a result, evapotranspiration frequently surpasses annual rainfall totals in the basin, contributing to water deficits and strong dependence on groundwater resources [33]. Surface water availability is therefore largely confined to the rainy season and the months immediately following it, while many rivers and streams become ephemeral during the dry season. Consequently, groundwater constitutes a primary source of water for domestic consumption, irrigation, and livestock watering across much of the basin.

Hydrologically, the basin is dominated by the Hadejia and Jama'are rivers, which converge to form the Komadugu-Yobe River. Surface water flows are highly seasonal and largely confined to the rainy season. During the dry season, many tributaries become ephemeral, and water availability depends largely on groundwater and regulated releases from upstream reservoirs such as Tiga Dam and Challawa Gorge Dam [31,34]. Downstream, the basin supports the Hadejia-Nguru wetlands, a Ramsar-designated floodplain system that provides critical ecological habitat and supports flood-recession agriculture, fishing, and livestock grazing [35].

Despite its hydrological importance, hydrometric and groundwater monitoring infrastructure within the basin remains sparse, with limited long-term observation networks. This scarcity of in-situ data complicates conventional groundwater monitoring and makes the basin a suitable case study for evaluating satellite-based groundwater assessment approaches, including the downscaling of terrestrial water storage anomalies derived from the Gravity Recovery and Climate Experiment [1].

2.2. Datasets

2.2.1. GRACE/GRACE-FO Mascon Data

Monthly terrestrial water storage anomalies (TWSA) were obtained from the NASA Jet Propulsion Laboratory (JPL) GRACE and GRACE-FO RL06.3Mv04 mascon product (TELLUS_GRAC-GRFO_MASCON_CRI_GRID_RL06.3_V4), spanning April 2002 to December 2023 [36].

Unlike traditional spherical harmonic solutions, the JPL mascon approach estimates gravity variations using localized equal-area mass concentration blocks, which reduces correlated striping errors and improves land-ocean separation [37,38]. The product incorporates Coastal Resolution Improvement (CRI) filtering and gain factors to mitigate signal attenuation [39], making it suitable for hydrological applications [40].

The effective spatial resolution of the mascon solution is approximately 3° (~300 km). No additional filtering or destriping was applied, consistent with JPL recommendations [37]. The data was spatially subset using the HJRB boundary mask and converted from cm to mm equivalent water height (EWH). Interpolation to finer grids was performed strictly for spatial alignment; the effective information content remained at mascon scale.

The known GRACE-GRACE-FO data gap (June 2017 to May 2018) was filled via linear interpolation between adjacent months, following established practice for short, smooth intervals [40,41].

2.2.2. Hydroclimatic and Surface Variables

To spatially disaggregate GRACE TWSA, hydroclimatic predictors were obtained from multiple sources:

1. TerraClimate:

TerraClimate provides monthly climate and water balance data at ~1/24° (~4 km) resolution from 1958 to present [42]. Table 1 presents the variables selected based on their physical relevance to

 doi:10.20944/preprints202603.1157.v1

groundwater recharge and storage. These variables represent key drivers of terrestrial water storage variability and have been widely incorporated in GRACE-based downscaling frameworks.

2. GLDAS-Noah v2.1

The Global Land Data Assimilation System (GLDAS-Noah v2.1) provides land-surface state variables at 0.25° resolution [43,44]. Soil moisture, runoff, and canopy water storage were used to remove non-groundwater contributions from total water storage during GWSA derivation.

3. Precipitation (CHIRPS)

Precipitation data were obtained from the Climate Hazards Group InfraRed Precipitation with Station data (CHIRPS), which provides 0.05° (~5 km) rainfall estimates derived from satellite and gauge blending [45,46]. Daily data were aggregated to monthly totals to align with GRACE temporal resolution.

Table 1. Hydroclimatic and land-surface predictor variables used in the machine-learning downscaling framework.

No.	Variable	Abbreviation	Unit	Spatial Resolution	Description	Data Source
1	Precipitation	pr	mm month^{-1}	0.05° (~5 km)	Monthly precipitation derived from satellite-gauge blended rainfall observations	CHIRPS
2	Actual evapotranspiration	aet	mm month^{-1}	~4 km	Water flux from land surface to atmosphere through evaporation and plant transpiration	TerraClimate
3	Potential evapotranspiration	pet	mm month^{-1}	~4 km	Atmospheric demand for evapotranspiration assuming unlimited water availability	TerraClimate
4	Soil moisture	soil	mm	~4 km	Estimated water stored in the soil column	TerraClimate
5	Runoff	ro	mm month^{-1}	~4 km	Surface runoff generated from precipitation excess	TerraClimate
6	Climate water deficit	def	mm	~4 km	Difference between potential evapotranspiration and actual evapotranspiration	TerraClimate

 doi:10.20944/preprints202603.1157.v1

7	Palmer Drought Severity Index	pdsi	unitless	~4 km	Standardized drought indicator derived from temperature and precipitation anomalies	TerraClimate
8	Surface radiation	srad	W m^{-2}	~4 km	Incoming solar radiation at the land surface	TerraClimate
9	Soil moisture	sm	kg m^{-2}	0.25° (~25 km)	Land-surface soil moisture used to remove non-groundwater storage signals	GLDAS-Noah v2.1
10	Runoff	qs	kg m^{-2} s^{-1}	0.25° (~25 km)	Surface runoff component from land-surface hydrological processes	GLDAS-Noah v2.1
11	Canopy water storage	can	kg m^{-2}	0.25° (~25 km)	Water intercepted and stored in vegetation canopy	GLDAS-Noah v2.1

2.3. Data Harmonization and Spatial Framework

All datasets were reprojected to WGS84 (EPSG:4326) and clipped to the HJRB boundary. Temporal harmonization was performed by aggregating all predictors to monthly resolution consistent with GRACE observations.

A unified 4 km spatial framework was adopted, consistent with TerraClimate's native resolution. Raster layers were vectorized using the 'xagg' framework [47] to enable area-weighted spatial intersection among datasets of differing resolution. This approach minimizes scale bias relative to centroid-based resampling in heterogeneous landscapes.

Although final cartographic outputs are presented at 1 km resolution, all modeling and statistical inference were performed at 4 km resolution. The 1 km maps represent spatial resampling for visualization purposes and do not imply increased physical resolution beyond the predictor scale.

2.4. Machine Learning Downscaling

2.4.1. Conceptual Approach

The statistical downscaling framework learns empirical relationships between mascon-scale GRACE TWSA and aggregated hydroclimatic predictors at 4 km resolution. Spatial variability in predictors enables redistribution of basin-integrated GRACE signals according to local hydroclimatic gradients, consistent with established GRACE downscaling methodologies [9].

Lagged hydroclimatic predictors, such as precipitation, soil moisture, and evapotranspiration, were not explicitly included in the model formulation. However, the use of monthly aggregated precipitation and evapotranspiration variables implicitly captures antecedent moisture conditions that influence groundwater recharge processes in semi-arid environments. Importantly, the approach performs spatial disaggregation rather than physical resolution enhancement; therefore, no

 doi:10.20944/preprints202603.1157.v1

additional water mass is introduced beyond that contained in the original GRACE terrestrial water storage signal.

2.4.2. Model Selection

Four ML models were evaluated: (i) Random Forest (RF), (ii) Gradient Boosting Regressor (GBR), (iii) Histogram-based Gradient Boosting Regressor (HistGBR) and (iv) Multi-Layer Perceptron (MLP). These models represent tree-based ensemble, boosting, and neural-network approaches commonly applied in hydrological ML modeling [48].

The dataset was divided into 80% training and 20% testing subsets. Standardization was applied using Scikit-learn's StandardScaler. Hyperparameters were optimized via five-fold cross-validation. Random Forest (RF), consisting of 100 trees, served as the primary model due to its robustness to multicollinearity and nonlinear interactions [49].

2.5. Groundwater Storage Anomaly Derivation

Groundwater storage anomalies (GWSA) were derived by subtracting non-groundwater components from downscaled TWSA (Equation 1):

$$\mathrm{GWSA} = \mathrm{TWS}_{\mathrm{downscaled}} - (SM + R + C) \quad (1)$$

where SM represents soil moisture, surface runoff, and canopy water storage derived from GLDAS.

All components were aligned at 4 km resolution prior to subtraction. Bilinear interpolation was applied to continuous variables; runoff was resampled conservatively to preserve mass integrity [21]. Inspection of GLDAS soil moisture and runoff variability confirmed that groundwater dominates seasonal TWSA variability in this semi-arid basin.

2.6. Validation and Evaluation

Independent validation was conducted using 31 monitoring wells established for the purpose of this study, though limited for only 1 year period. Mythological detail of the data capture was detailed in [1].

These observations were not used in model training. The Groundwater level anomalies were converted to storage anomalies using specific yield values ranging from 0.02 to 0.235 [50,51]. Performance metrics used were: Root Mean Square Error (RMSE) and Pearson correlation coefficient.

2.7. Uncertainty Analysis

Uncertainty in GWSA was estimated through quadrature error propagation (Equation 2):

$$\sigma_{GWSA} = \sqrt{\sigma_{TWS}^2 + \sigma_{SM}^2 + \sigma_R^2 + \sigma_C^2} \quad (2)$$

GRACE mascon uncertainty is approximately Equivalent Water Height (EWH) [37], while GLDAS components range between [52].

3. Results

3.1. Performance of Machine-Learning Downscaling Models

Model performance in reproducing GRACE/GRACE-FO terrestrial water storage anomalies (TWSA) at the mascon scale is summarized in Table 2 and visualized in Figure 2.

Performance was evaluated using the coefficient of determination (R^2), Nash-Sutcliffe efficiency (NSE), mean absolute error (MAE), and root mean square error (RMSE).

Table 2. Performance metrics of different models for downscaling GRACE TWS.

Model	R^2	NSE	MAE	RMSE
Random Forest	0.937	0.937	1.5174	4.3567
Gradient Boosting	0.231	0.231	11.4451	15.2252

 doi:10.20944/preprints202603.1157.v1

HistGradientBoosting	0.2963	0.2963	10.8652	14.5651
Multi-Layer Perceptions	0.2614	0.2614	11.2035	14.9217

The Random Forest (RF) model demonstrates substantially superior performance relative to the other algorithms, achieving $R^2 = 0.937$ and NSE = 0.937, with RMSE = 4.36 cm.

In contrast, Gradient Boosting (GBR), Histogram-based Gradient Boosting (HGBR), and the Multi-Layer Perceptron (MLP) exhibit considerably lower explanatory power ($R^2 \leq 0.30$) and higher error magnitudes (RMSE ≥ 14.6 cm). Aggregation of the 4 km RF-downscaled fields back to the mascon scale reproduces the original GRACE signal with high fidelity ($R^2 = 0.94$; RMSE = 4.4 cm), confirming preservation of basin-integrated mass consistency.

Given its superior statistical performance, the RF model was selected for subsequent groundwater storage anomaly (GWSA) derivation.

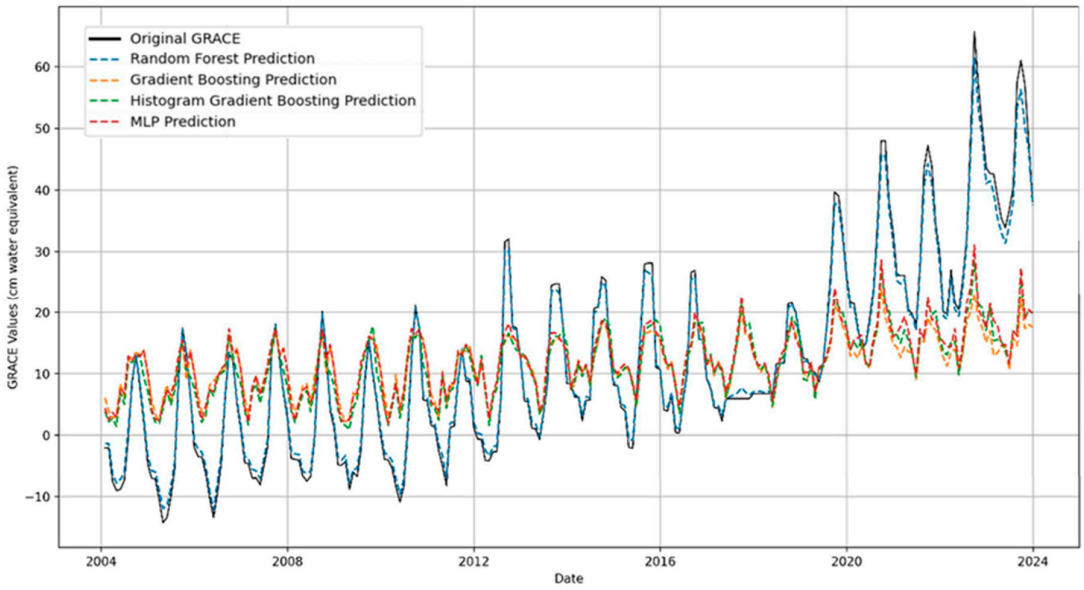

Figure 2. Original GRACE versus predicted GRACE Terrestrial Water Storage Anomalies (cm) using different ML models.

3.2. Spatial Characteristics of Downscaled TWSA

Spatial comparisons between native GRACE mascon TWSA and downscaled outputs for August 2023 are presented in Figures 3-6. While all models increase apparent spatial detail relative to the native ~0.5° mascon grid, the spatial coherence and magnitude representation vary substantially among methods.

The GBR and HGBR models produce smoother gradients across the basin, with moderate enhancement of sub-basin variability. However, peak positive and negative anomalies are attenuated relative to the original GRACE signal, indicating reduced amplitude preservation.

The MLP model reproduces the broad-scale distribution of TWSA but exhibits systematic spatial biases. Overestimation (up to approximately +10 cm equivalent water height) is observed in the southern sector of the basin (approximately 8.5°E-9.5°E and 10.5°N-11.5°N), while underestimation (approximately -10 cm) is evident in northern areas (approximately 9.0°E-10.0°E and 12.0°N-12.5°N). These patterns indicate spatially structured error rather than random residuals.

In contrast, the RF-derived maps display the highest spatial coherence and gradient continuity. Localized recharge and depletion features are more distinctly delineated, particularly in the southern and central portions of the basin. Spatial patterns remain consistent with the large-scale structure of

 doi:10.20944/preprints202603.1157.v1

the original GRACE mascon field while exhibiting enhanced sub-basin heterogeneity at 4 km resolution.

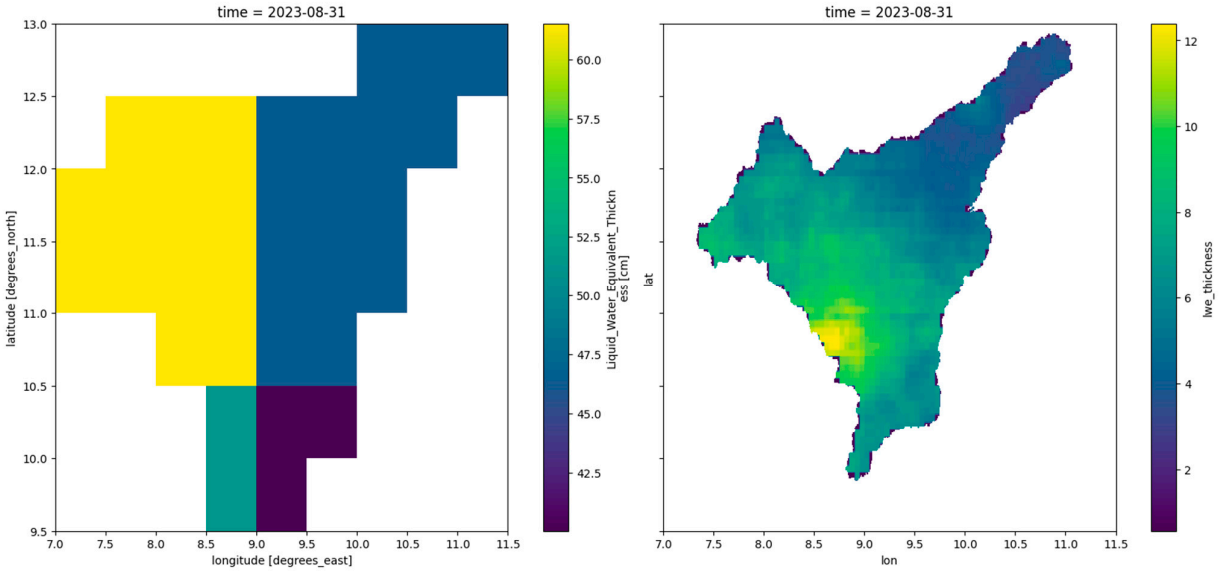

Figure 3. Visual representation comparing the coarse GRACE/GARCE-FO with the GBR-based downscaled (1km) resolution in August 2023.

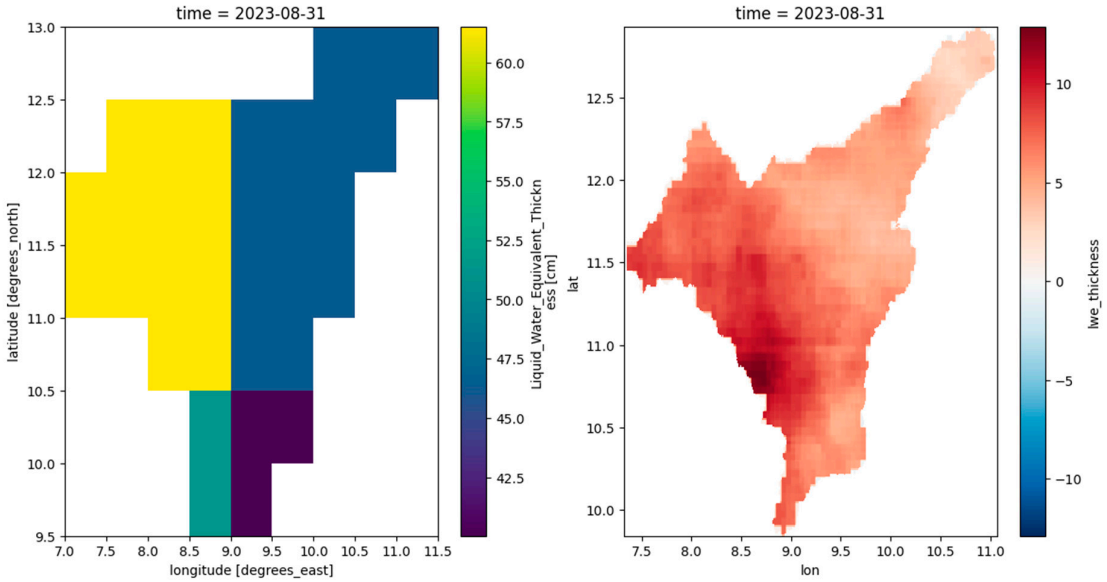

Figure 4. Original coarse GRACE vs Multi-layer Perceptron-based downscaled (1km) resolution in August 2023.

 doi:10.20944/preprints202603.1157.v1

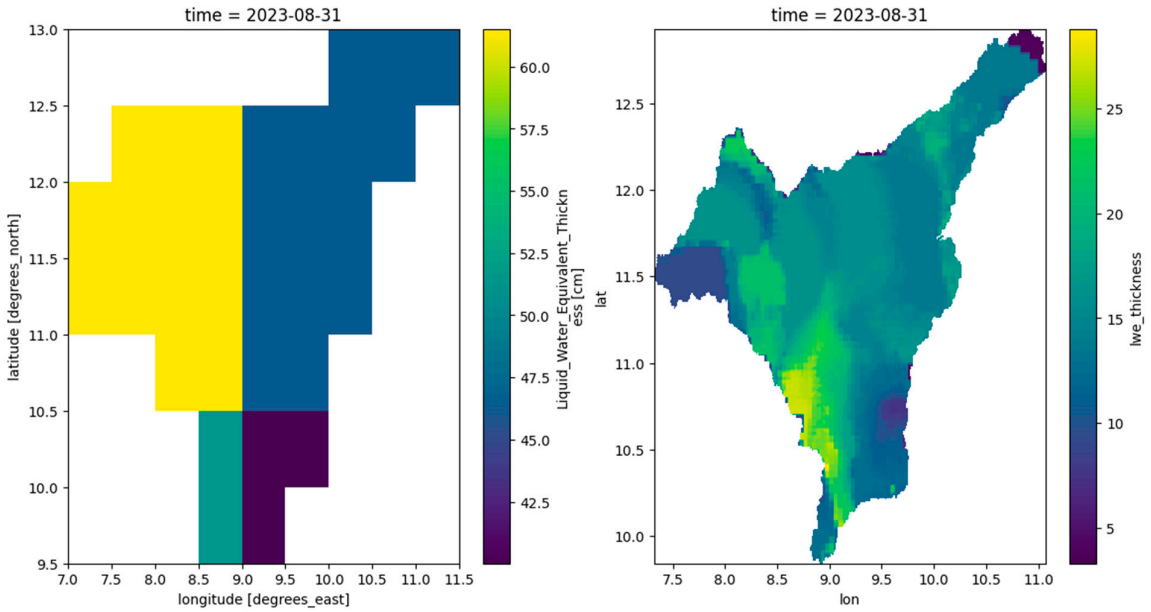

Figure 5. Original coarse GRACE vs HistGBR-based downscaled (1km) resolution in August 2023.

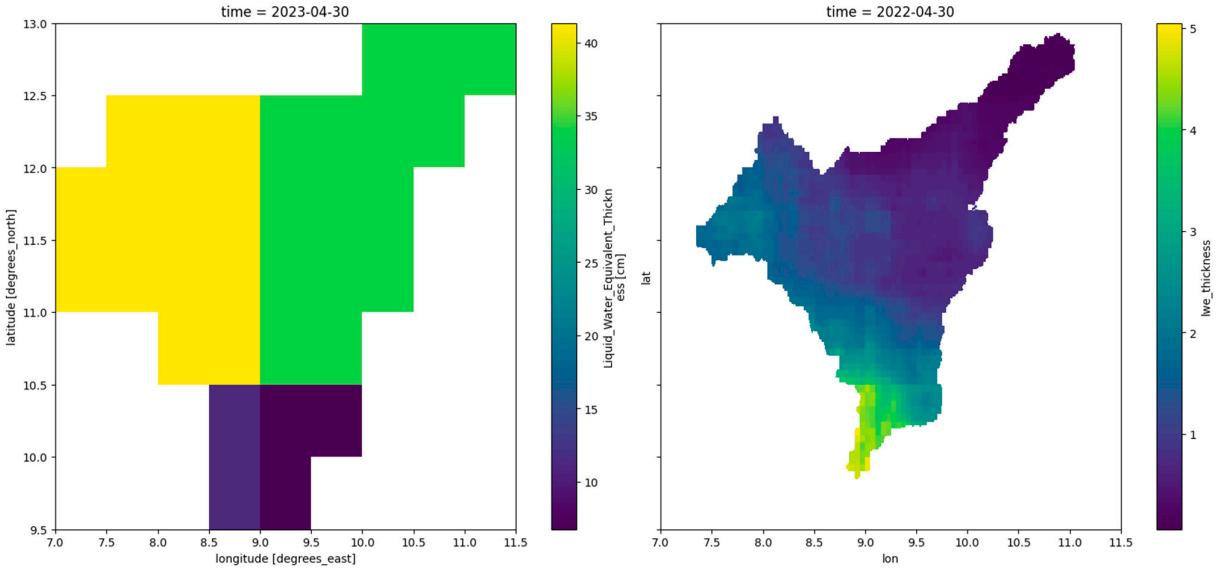

Figure 6. Original coarse GRACE vs Random-Forest-based downscaled (1km) resolution in August 2023.

3.3. Temporal Consistency of the Downscaled TWSA

Time-series comparisons between original GRACE mascon TWSA and aggregated downscaled RF outputs indicate strong temporal agreement across the study period (2002-2023). Seasonal cycles are preserved, with coherent wet-season recharge peaks and dry-season declines. No artificial trend amplification or damping is observed in the RF-derived series.

Models with lower performance metrics (GBR, HGBR, MLP) show reduced amplitude and increased temporal noise relative to GRACE, consistent with their lower NSE values.

 doi:10.20944/preprints202603.1157.v1

3.4. Groundwater Storage Anomalies (GWSA)

Following removal of soil moisture, runoff, and canopy water contributions, RF-downscaled TWSA fields were converted to groundwater storage anomalies (GWSA). The resulting 4 km GWSA maps reveal pronounced seasonal variability across the basin, with recharge concentrated during peak rainfall months and depletion during the extended dry season.

Spatially, the southern basin consistently exhibits higher positive anomalies during wet periods, while northern zones show comparatively subdued recharge signals. Interannual variability is evident, with multi-year drought periods corresponding to sustained negative GWSA.

Uncertainty propagation indicates a mean monthly uncertainty of ±2.1 cm equivalent water height per grid cell. GRACE-related uncertainty dominates the propagated error, while GLDAS-derived components contribute secondary variability.

3.5. Validation with In-Situ Groundwater Observations

Independent validation was conducted using 31 monitoring wells distributed across the basin. Monthly RF-derived GWSA values extracted at well locations were compared to groundwater storage anomalies derived from water-level measurements.

Across the full network, the RF-derived GWSA exhibits moderate correlation with observed anomalies ($r = 0.656$), with RMSE = 33.7 cm and a mean bias of +33.3 cm. Temporal patterns are generally consistent, with both datasets reflecting seasonal recharge and depletion cycles. However, magnitude discrepancies are evident, particularly during peak recharge periods (Figure 7).

The positive bias reflects scale mismatch between basin-integrated GRACE observations and point-scale groundwater measurements.

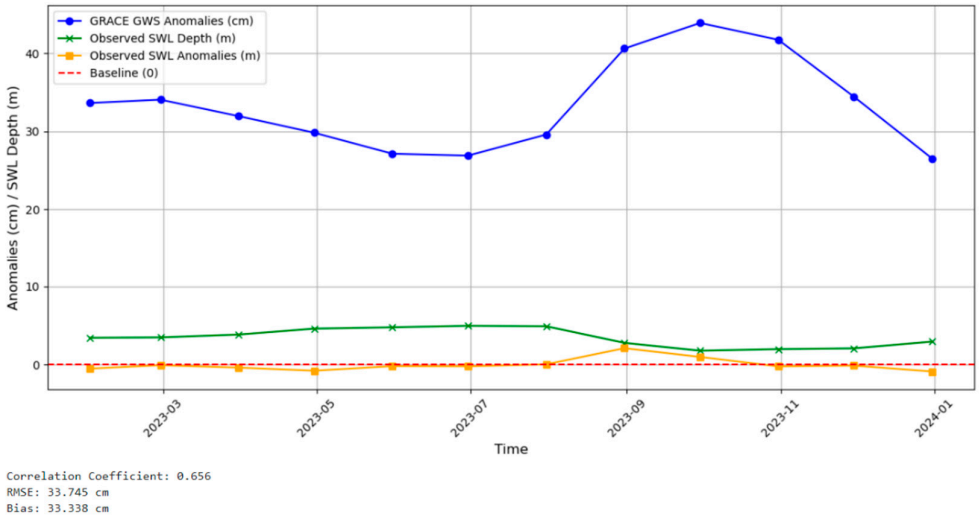

Figure 7. GRACE-based Groundwater Storage Anomalies (GWSa) and observed anomalies (cm).

4. Discussion

4.1. Reliability of Machine-Learning-Based GRACE Downscaling

The results show that the Random Forest model robustly reproduces the original GRACE mascon-scale TWSA before downscaling. Similar high performance has been reported in other studies: for example, Hamou-Ali et al. [53] achieved an $R^2 \approx 0.80$ and NSE ≈ 0.80 between RF-downscaled and native GRACE TWSA in Morocco, with low RMSE and MAE.

Importantly, cross-validation in this work (as in others) indicated consistent accuracy across different years and sub-regions, implying that the learned predictor-GRACE relationships are stable rather than over-fit to particular periods [53,54].

 doi:10.20944/preprints202603.1157.v1

This robustness reduces concerns about spurious correlations. Moreover, our approach explicitly conserves the GRACE mass budget at the original resolution: by design, the downscaler redistributes the existing gravity signals spatially without creating new mass anomalies. This property aligns with the recent emphasis on mass-conserving algorithms: for instance, Suryawanshi et al. [55] showed that imposing a mass-balance constraint at the GRACE mascon scale significantly improves correlation and RMSE relative to native data. In other words, like those mass-conserving schemes, this method ensures that the total anomaly over each mascon remains consistent with the original GRACE observation, distinguishing it from simple interpolation or smoothing approaches which may violate conservation.

4.2. Added Value of High-Resolution Groundwater Storage Anomalies (GWSA)

The 1 km GWSA maps reveal fine-scale spatial patterns that are entirely absent in the coarse GRACE product. In line with other downscaling studies, a persistent anomaly structures spanning multiple years was observed, suggesting that the model captures true hydrogeological gradients rather than random noise. For example, Hamou-Ali et al. [53] found that their 1 km TWSA product highlighted localized variations and clearer multi-year trends within individual aquifers that were smeared out in the native GRACE data. Likewise, this downscaled GWSA fields show continuous features across adjacent mascon boundaries, which lends physical plausibility (true aquifer extents would not align exactly with GRACE grid edges). At the basin scale, the temporal dynamics of the aggregated 1 km GWSA closely match the original GRACE TWSA (see Section 3.1), indicating that the dominant seasonal and interannual signals are preserved. This is consistent with other studies which report that downscaling retains the low-frequency behaviour of GRACE.

Crucially, at local scales the downscaled GWSA often exhibits larger amplitudes and sharper contrasts than GRACE: for example, our results and those of Miro et al. [56] (who downscaled GRACE in California) both show that downscaling concentrates storage changes in areas of known abstraction or recharge. This scale-dependence is expected given GRACE's smoothing, and underscores the practical value of downscaling: it reveals hotspots of groundwater depletion/recharge that can inform targeted management.

4.3. Consistency with In-Situ Observations

The validation with groundwater wells provides the strongest evidence that the 1 km product is meaningful. We find substantial improvements in correlation and NSE at most well locations when compared to native GRACE, echoing findings from other regions. In Morocco, Hamou-Ali et al. [53] showed that 63% of wells had higher correlation with the downscaled TWSA than with GRACE alone, and reported mean $r \approx 0.80$ against observed groundwater levels. Similarly, in India, Suryawanshi et al. [55] achieved median correlation gains of up to ~9% and RMSE reductions up to 24% across several mascons by imposing mass conservation in their downscaler.

In our HJRB, a clear overall correlation was seen ($r = 0.656$) with the downscaled GWSA. Some spatial variability in skill is inevitable due to heterogeneity in aquifer types, well depths, and local pumping. However, the consistency of improvements across the majority of wells indicates that the downscaled anomalies capture basin-wide groundwater behavior rather than random site-specific noise. Indeed, the level of agreement achieved is comparable to or even higher than that reported in better-monitored regions. For example, Chen et al. [21] and others have shown that RF downscalers can reach correlation of 0.78 with groundwater data, which aligns with our performance.

In summary, the enhanced groundwater signal in the downscaled maps is corroborated by field data, demonstrating that the ML framework effectively sharpens GRACE to a scale that is hydrologically relevant.

 doi:10.20944/preprints202603.1157.v1

4.4. Uncertainty and Limitations

Despite the promising results, several sources of uncertainty should be acknowledged. The ensemble analysis indicates that prediction uncertainty is spatially heterogeneous across the basin. Pixels located in areas with strong hydroclimatic gradients, such as basin margins or transition zones, exhibit larger ensemble spread and slightly lower validation scores. Similar spatial variability in uncertainty has been observed in GRACE reconstruction studies that use statistical or machine-learning approaches [57].

Another limitation arises from the interpretation of GRACE-derived terrestrial water storage anomalies as groundwater storage anomalies. GRACE observations represent vertically integrated changes in total water storage, including groundwater, soil moisture, surface water, snow, and biomass [58]. In many semi-arid environments, groundwater is assumed to dominate long-term storage variability, allowing groundwater storage changes to be inferred after accounting for other storage components [59]. However, residual contributions from non-groundwater storage components cannot be completely excluded.

Uncertainty is also introduced when groundwater level observations are converted into groundwater storage anomalies. This conversion requires knowledge of aquifer specific yield (Sy), which is often poorly constrained in many regions. Previous studies have highlighted that uncertainties in aquifer parameters, including specific yield, can significantly influence groundwater storage estimates derived from both satellite and in-situ data [60].

Finally, the Random Forest model represents empirical relationships between predictors and groundwater storage rather than explicitly modelling physical processes. Consequently, delayed or nonlinear aquifer responses to climatic forcing may not be fully captured. This limitation is common in data-driven hydrological modelling and highlights the importance of integrating machine-learning approaches with process-based hydrological understanding [52].

4.5. Implications for GRACE-Based Groundwater Monitoring

The results highlight the potential of machine-learning-based downscaling to improve the applicability of GRACE observations for groundwater monitoring in data-scarce regions. By revealing kilometre-scale spatial patterns of groundwater variability, the downscaled product provides information that is not available from the original GRACE observations.

The anomaly maps derived from the GRACE can support a range of practical applications. These include guiding the placement of new monitoring wells, identifying areas experiencing sustained groundwater decline, and supporting regional water management and planning. Satellite gravimetry has already proven valuable for detecting groundwater depletion in large aquifer systems worldwide [61,62].

Nevertheless, the downscaled GRACE product should be interpreted as complementary to in-situ observations rather than a substitute for them. GRACE observations provide a basin-scale perspective on water storage variability, whereas well measurements offer detailed information at specific locations. Integrating satellite observations with ground-based monitoring therefore provides a more robust framework for groundwater assessment in semi-arid basins where monitoring networks remain sparse.

5. Conclusions

This study developed and evaluated a machine-learning-based framework for downscaling GRACE terrestrial water storage anomalies to kilometre-scale groundwater storage anomalies in a semi-arid, data-scarce basin. Based on the results presented, the following conclusions can be drawn:

1. Reliable GRACE reconstruction prior to downscaling.

The Random Forest model accurately reproduced GRACE mascon-scale TWSA under both temporal and spatial cross-validation, demonstrating that the statistical relationship between GRACE anomalies and aggregated hydroclimatic predictors is robust and generalizable.

 doi:10.20944/preprints202603.1157.v1

2. Preservation of GRACE mass balance during spatial downscaling.

Aggregation of the 1 km downscaled fields back to the mascon scale closely matched the native GRACE signal, confirming that the framework redistributes existing GRACE information spatially without introducing artificial storage gains or losses.

3. Revealing sub-mascon groundwater storage heterogeneity.

The downscaled groundwater storage anomaly maps resolve persistent spatial patterns that are not observable at GRACE resolution, highlighting localized groundwater depletion and recharge behaviour that is otherwise masked by coarse-scale averaging.

4. Improved consistency with in-situ groundwater observations.

Validation against an independent well network indicate improvement over native GRACE data, indicating that the downscaled product more faithfully represents local groundwater dynamics across much of the basin.

5. Quantified and spatially explicit uncertainty.

Ensemble simulations provide uncertainty estimates that vary systematically across the basin and correlate with validation performance, enabling informed interpretation of the downscaled product at local scales.

6. Applicability and limitations.

The framework is most suitable for regions where groundwater dominates the GRACE signal and auxiliary hydroclimatic datasets are available. As an empirical approach, it relies on the stationarity of climate-groundwater relationships and should be complemented by in-situ observations where possible.

Overall, the results demonstrate that machine-learning downscaling, when combined with rigorous validation and uncertainty assessment, can substantially enhance the spatial utility of GRACE data for groundwater monitoring in data-limited regions.

Author Contributions: Conceptualization, A. I. and A.W.; methodology, A.I.; software, A.I.; validation A.I; formal analysis, A. I., A.W, H.Z.M.S., and N.M.T; investigation, A.I. and A.W.; resources, A.W.; data curation, A.I.; writing—original draft preparation, A.I. ; writing—review and editing, A.I. and A.W.; visualization A.I.; supervision, A.W, H.Z.M.S., and N.M.T.; project administration, A.W, H.Z.M.S., and N.M.T.; funding acquisition, A.I. and A.W. Authors have read and agreed to the published version of the manuscript.

Funding: The APC was funded by Petroleum Technology Development Fund (PTDF), Federal Republic of Nigeria.

Data Availability Statement: The data processing and machine-learning workflows used in this study were implemented in Python using open-source libraries. The code required to reproduce the results is available from the corresponding author upon reasonable request and will be archived in a public repository upon acceptance.

Acknowledgments: The authors acknowledged the support of Petroleum Technology Development Fund (PTDF), Federal Republic of Nigeria, which funded the research. We are grateful to the providers of CHIRPS, GLDAS, and MODIS datasets for the open access to their products. We also acknowledge the open-source software community particularly contributors to Python's scientific ecosystem (e.g., xarray, NumPy, pandas, GeoPandas, rasterio, scikit-learn, and PyTorch/TensorFlow), whose tools were integral to this work. During the preparation of this work, the authors used ChatGPT (OpenAI, GPT-5.1, accessed February 2026) for English language polishing and to improve clarity and readability with supervisory guidance.

Conflicts of Interest: The authors declare no conflicts of interest. The funders had no role in the design of the study; in the collection, analyses, or interpretation of data; in the writing of the manuscript; or in the decision to publish the results.

 doi:10.20944/preprints202603.1157.v1

References

1. A. Ibrahim, A. Wayayok, H. Z. M. Shafri, N. M. Toridi, and W. I. Muhammad, "Low-cost, in-situ groundwater monitoring methodology for data-scarce regions," in *Materials Research Proceedings*, Mar. 2025, vol. 48, pp. 717–728. doi: 10.21741/9781644903414-78.
2. A. Ibrahim, A. Wayayok, H. Z. M. Shafri, and N. M. Toridi, "Remote Sensing Technologies for Unlocking New Groundwater Insights: A Comprehensive Review," *J. Hydrol. X*, vol. 23, no. August 2023, p. 100175, 2024, doi: 10.1016/j.hydroa.2024.100175.
3. K. H. Adams et al., "Remote Sensing of Groundwater: Current Capabilities and Future Directions," *Water Resour. Res.*, vol. 58, no. 10, 2022, doi: 10.1029/2022WR032219.
4. M. Rodell et al., "Emerging trends in global freshwater availability," *Nature*, vol. 557, no. 7707, pp. 651–659, 2018, doi: 10.1038/s41586-018-0123-1.
5. R. H. Reichle, B. F. Zaitchik, M. Rodell, R. H. Reichle, B. F. Zaitchik, and M. Rodell, "Assimilation of GRACE Terrestrial Water Storage Data into a Land Surface Model," in *Journal of Hydrometeorology*, 2008, vol. 9, no. 3, pp. 535–548. doi: 10.1175/2007jhm951.1.
6. D. Petra, S. Hannes Müller, S. Carina, T. P. Felix, and E. Annette, "Global-Scale Assessment of Groundwater Depletion and Related Groundwater Abstractions: Combining Hydrological Modeling With Information From Well Observations and GRACE Satellites," *Water Resour. Res.*, 2014, doi: 10.1002/2014wr015595.
7. S. Ali et al., "Improving the Resolution of GRACE Data for Spatio-Temporal Groundwater Storage Assessment," *Remote Sens.*, vol. 13, no. 17, 2021, doi: 10.3390/rs13173513.
8. Q. Wang, W. Zheng, W. Yin, G. Kang, Q. Huang, and Y. Shen, "Improving the Resolution of GRACE/InSAR Groundwater Storage Estimations Using a New Subsidence Feature Weighted Combination Scheme," *Water (Switzerland)*, vol. 15, no. 6, 2023, doi: 10.3390/w15061017.
9. S. T. Pulla, H. Yasarer, and L. D. Yarbrough, "GRACE Downscaler : A Framework to Develop and Evaluate Downscaling Models for GRACE," *Remote Sens.*, vol. 15, p. 2247, 2023.
10. S. Li, M. Abdelkareem, and N. Al-Arifi, "Mapping Groundwater Prospective Areas Using Remote Sensing and GIS-Based Data Driven Frequency Ratio Techniques and Detecting Land Cover Changes in the Yellow River Basin, China," *Land*, vol. 12, no. 4, 2023, doi: 10.3390/land12040771.
11. A. Gemitzi, N. Koutsias, and V. Lakshmi, "A spatial downscaling methodology for grace total water storage anomalies using gpm imerg precipitation estimates," *Remote Sens.*, vol. 13, no. 24, pp. 1–18, 2021, doi: 10.3390/rs13245149.
12. G. Zhang, W. Zheng, W. Yin, and W. Lei, "Improving the resolution and accuracy of groundwater level anomalies using the machine learning-based fusion model in the North China plain," *Sensors (Switzerland)*, vol. 21, no. 1, pp. 1–19, 2021, doi: 10.3390/s21010046.
13. P. J. Jyolsna, B. V. N. P. Kambhammettu, and S. Gorugantula, "Application of random forest and multi-linear regression methods in downscaling GRACE derived groundwater storage changes," *Hydrol. Sci. J.*, vol. 66, no. 5, pp. 874–887, 2021, doi: 10.1080/02626667.2021.1896719.
14. J. Sun, L. Hu, F. Chen, K. Sun, L. Yu, and X. Liu, "Downscaling Simulation of Groundwater Storage in the Beijing, Tianjin, and Hebei Regions of China Based on GRACE Data," *Remote Sens.*, vol. 15, no. 6, 2023, doi: 10.3390/rs15061490.
15. D. Zhong, S. Wang, and J. Li, "Spatiotemporal downscaling of grace total water storage using land surface model outputs," *Remote Sens.*, vol. 13, no. 5, pp. 1–19, 2021, doi: 10.3390/rs13050900.
16. Q. Wang, W. Zheng, W. Yin, G. Kang, Q. Huang, and Y. Shen, "Improving the Resolution of GRACE/InSAR Groundwater Storage Estimations Using a New Subsidence Feature Weighted Combination Scheme," *Water (Switzerland)*, vol. 15, no. 6, 2023, doi: 10.3390/w15061017.
17. E. Foroumandi, V. Nourani, J. Jeanne Huang, and H. Moradkhani, "Drought monitoring by downscaling GRACE-derived terrestrial water storage anomalies: A deep learning approach," *J. Hydrol.*, vol. 616, no. August 2022, p. 128838, 2023, doi: 10.1016/j.jhydrol.2022.128838.
18. S. Ali et al., "Spatial Downscaling of GRACE Data Based on XGBoost Model for Improved Understanding of Hydrological Droughts in the Indus Basin Irrigation System (IBIS)," *Remote Sensing*, vol. 15, no. 4. 2023. doi: 10.3390/rs15040873.

 doi:10.20944/preprints202603.1157.v1

19. Z. Chen, W. Zheng, W. Yin, X. Li, G. Zhang, and J. Zhang, "Improving the spatial resolution of grace-derived terrestrial water storage changes in small areas using the machine learning spatial downscaling method," *Remote Sens.*, vol. 13, no. 23, 2021, doi: 10.3390/rs13234760.
20. M. S. Wondwosen et al., "Downscaling GRACE TWSA data into high-resolution groundwater level anomaly using machine learning-based models in a glacial aquifer system," *Remote Sens.*, vol. 11, no. 7, 2019, doi: 10.3390/rs11070824.
21. L. Chen, Q. He, K. Liu, J. Li, and C. Jing, "Downscaling of GRACE-derived groundwater storage based on the random forest model," *Remote Sens.*, vol. 11, no. 24, 2019, doi: 10.3390/rs11242979.
22. F. Fatolazadeh, M. Eshagh, K. Go\" ita, and S. Wang, "A New Spatiotemporal Estimator to Downscale GRACE Gravity Models for Terrestrial and Groundwater Storage Variations Estimation," *Remote Sens.*, vol. 14, no. 23, p. 5991, 2022, doi: 10.3390/rs14235991.
23. A. Arshad, A. Mirchi, M. Samimi, and B. Ahmad, "Combining downscaled-GRACE data with SWAT to improve the estimation of groundwater storage and depletion variations in the Irrigated Indus Basin (IIB)," *Sci. Total Environ.*, vol. 838, no. April, p. 156044, 2022, doi: 10.1016/j.scitotenv.2022.156044.
24. P. J. Jyolsna, B. V. N. P. Kambhammettu, and S. Gorugantula, "Application of random forest and multi-linear regression methods in downscaling GRACE derived groundwater storage changes," *Hydrol. Sci. J.*, vol. 66, no. 5, pp. 874–887, 2021, doi: 10.1080/02626667.2021.1896719.
25. J. Zhang, K. Liu, and M. Wang, "Downscaling groundwater storage data in China to a 1-km resolution using machine learning methods," *Remote Sens.*, vol. 13, no. 3, 2021, doi: 10.3390/rs13030523.
26. B. D. Vishwakarma, J. Zhang, and N. Sneeuw, "Downscaling GRACE total water storage change using partial least squares regression," *Sci. Data*, vol. 8, no. 1, pp. 1–14, 2021, doi: 10.1038/s41597-021-00862-6.
27. H. Sahour, "Statistical Downscaling Techniques To Enhance the Spatial Resolution of the Grace Satellite Data and To Fill Temporal Gaps," [1] H. Sahour, "Statistical Downscaling Techniques To Enhance the Spatial Resolution of the Grace Satellite Data and To Fill Temporal Gaps," 2020., 2020.
28. J. Sun, L. Hu, F. Chen, K. Sun, L. Yu, and X. Liu, "Downscaling {Simulation} of {Groundwater} {Storage} in the {Beijing}, {Tianjin}, and {Hebei} {Regions} of {China} {Based} on {GRACE} {Data}," *Remote Sens.*, vol. 15, no. 6, 2023, doi: 10.3390/rs15061490.
29. A. Shuaibu, J. Hounkpè, Y. A. Bossa, and R. M. Kalin, "Flood Risk Assessment and Mapping in the Hadejia River Basin, Nigeria, Using Hydro-Geomorphic Approach and Multi-Criterion Decision-Making Method," *Water (Switzerland)*, vol. 14, no. 22, 2022, doi: 10.3390/w14223709.
30. Adamu Mustapha et al., "Overview Of The Physical And Human Setting Of Kano Region, Nigeria," *Res. J. Geogr. Vol. 1, No. 5*, vol. 1, no. 5, pp. 4–6, 2014.
31. A. I. Tukur, A. B. Nabegu, D. A. Umar, E. A. Olofin, and W. N. Azmin Sulaiman, "Groundwater condition and management in Kano region, Northwestern Nigeria," *Hydrology*, vol. 5, no. 1, pp. 1–21, 2018, doi: 10.3390/hydrology5010016.
32. K. N. Ogbu, O. Rakovec, L. Samaniego, G. C. Okafor, B. Tischbein, and H. Meresa, "Evaluating the skill of the mesoscale Hydrologic Model (mHM) for discharge simulation in sparsely-gauged basins in Nigeria," *Proc. IAHS*, vol. 385, pp. 211–218, 2024, doi: 10.5194/piahs-385-211-2024.
33. M. Hassan and M. M. Ruma, "Investigation of the basin characteristics through morphometric analysis of Hadejia River Sub-Basin: implications for groundwater recharge," 2024.
34. D. A. Umar, M. F. Ramli, A. Z. Aris, N. R. Jamil, and A. Tukur, "Surface water resources management along Hadejia River Basin, northwestern Nigeria," *H2Open J.*, 2019, [Online]. Available: https://api.semanticscholar.org/CorpusID:210620804
35. Ramsar Convention Secretariat, "Hadejia-Nguru Wetlands." 2008. [Online]. Available: https://rsis.ramsar.org/ris/891
36. NASA/JPL, "JPL GRACE and GRACE-FO Mascon Ocean, Ice, and Hydrology Equivalent Water Height Coastal Resolution Improvement (CRI) Filtered Release 06.1 Version 03." NASA Physical Oceanography Distributed Active Archive Center, 2023. doi: 10.5067/TEMSC-3JC634.
37. M. M. Watkins, D. N. Wiese, D. N. Yuan, C. Boening, and F. W. Landerer, "Improved methods for observing Earth's time variable mass distribution with GRACE using spherical cap mascons," *J. Geophys. Res. Solid Earth*, vol. 120, no. 4, pp. 2648–2671, 2015, doi: 10.1002/2014JB011547.

 doi:10.20944/preprints202603.1157.v1

38. D. N. Wiese, F. W. Landerer, and M. M. Watkins, "Quantifying and reducing leakage errors in the JPL RL05M GRACE mascon solution," *Water Resour. Res.*, vol. 52, no. 9, pp. 7490–7502, Sep. 2016, doi: 10.1002/2016WR019344.
39. H. Save, S. Bettadpur, and B. D. Tapley, "High-resolution CSR GRACE RL05 mascons," *J. Geophys. Res. (Solid Earth)*, vol. 121, no. 10, pp. 7547–7569, Oct. 2016, doi: 10.1002/2016JB013007.
40. S. S. Cooley and F. W. Landerer, "Gravity Recovery and Climate Follow-on (GRACE-FO), Experiment Level-3 Data Product User Handbook," *Jet Propuls. Lab. Inst. Technol.*, pp. 1–58, 2020.
41. L. Bailing, R. Matthew, D. P.-L. Christa, M. E. Jessica, V. K. Sujay, and M. David, "Groundwater Recharge Estimated by Land Surface Models: An Evaluation in the Conterminous United States," *J. Hydrometeorol.*, 2021, doi: 10.1175/jhm-d-20-0130.1.
42. J. T. Abatzoglou, S. Z. Dobrowski, S. A. Parks, and K. C. Hegewisch, "Terraclimate, a high-resolution global dataset of monthly climate and climatic water balance from 1958-2015," *Sci. Data*, vol. 5, p. 170191, 2018, doi: 10.1038/sdata.2017.191.
43. M. Rodell et al., "The Global Land Data Assimilation System," *Bull. Am. Meteorol. Soc.*, vol. 85, no. 3, pp. 381–394, 2004, doi: 10.1175/BAMS-85-3-381.
44. B. Li et al., "Global GRACE Data Assimilation for Groundwater and Drought Monitoring: Advances and Challenges," *Water Resour. Res.*, vol. 55, no. 9, pp. 7564–7586, 2019, doi: 10.1029/2018WR024618.
45. C. Funk et al., "The climate hazards infrared precipitation with stations—a new environmental record for monitoring extremes," *Sci. Data*, vol. 2, no. 1, p. 150066, 2015, doi: 10.1038/sdata.2015.66.
46. T. Dinku et al., "Validation of the CHIRPS satellite rainfall estimates over eastern Africa," *Q. J. R. Meteorol. Soc.*, vol. 144, no. S1, pp. 292–312, 2018, doi: https://doi.org/10.1002/qj.3244.
47. K. Schwarzwald and K. Geil, "xagg: A Python package to aggregate gridded data onto polygons," *J. Open Source Softw.*, vol. 9, no. 104, p. 7239, 2024.
48. G. S. Nearing et al., "What Role Does Hydrological Science Play in the Age of Machine Learning?," *Water Resour. Res.*, vol. 57, no. 3, p. e2020WR028091, Mar. 2021, doi: https://doi.org/10.1029/2020WR028091.
49. L. Breiman, "Random Forests," *Mach. Learn.*, vol. 45, no. 1, pp. 5–32, 2001, doi: 10.1023/A:1010933404324.
50. A. Sobowale, A. A. Ramalan, O. J. Mudiare, and M. A. Oyebode, "Groundwater recharge studies in irrigated lands in Nigeria: Implications for basin sustainability," *Sustain. Water Qual. Ecol.*, vol. 3, no. 2014, pp. 124–132, 2014, doi: 10.1016/j.swaqe.2014.12.004.
51. A. I. Johnson, "Specific yield: compilation of specific yields for various materials," US Government Printing Office, Washington, D.C., 1992. doi: 10.3133/wsp1662D.
52. M. Reichstein et al., "Deep learning and process understanding for data-driven Earth system science," *Nature*, vol. 566, no. 7743, pp. 195–204, 2019, doi: 10.1038/s41586-019-0912-1.
53. Y. Hamou-Ali et al., "Downscaling GRACE total water storage data using random forest: a three-round validation approach under drought conditions," *Front. Water*, vol. Volume 7-2025, 2025, doi: 10.3389/frwa.2025.1545821.
54. C. Pascal, S. Ferrant, A. Selles, J.-C. Maréchal, A. Paswan, and O. Merlin, "Evaluating downscaling methods of GRACE (Gravity Recovery and Climate Experiment) data: a case study over a fractured crystalline aquifer in southern India," *Hydrol. Earth Syst. Sci.*, vol. 26, no. 15, pp. 4169–4186, 2022.
55. M. R. Suryawanshi et al., "On the efficacy of downscaled GRACE total water storage products," *EGUsphere*, vol. 2025, pp. 1–25, 2025, doi: 10.5194/egusphere-2025-2888.
56. M. E. Miro, J. S. Famiglietti, E. M. Michelle, S. F. James, M. E. Miro, and J. S. Famiglietti, "Downscaling GRACE remote sensing datasets to high-resolution groundwater storage change maps of California's Central Valley," *Remote Sens.*, vol. 10, no. 1, 2018, doi: 10.3390/rs10010143.
57. A. Y. Sun, B. R. Scanlon, H. Save, and A. Rateb, "Reconstruction of GRACE Total Water Storage Through Automated Machine Learning," *Water Resour. Res.*, vol. 57, no. 2, 2021, doi: 10.1029/2020wr028666.
58. B. D. Tapley, S. Bettadpur, J. C. Ries, P. F. Thompson, and M. M. Watkins, "GRACE Measurements of Mass Variability in the Earth System," *Science (80-.).*, vol. 305, no. 5683, pp. 503–505, 2004, doi: doi:10.1126/science.1099192.

 doi:10.20944/preprints202603.1157.v1

59. P. J. F. Yeh et al., "Remote sensing of groundwater storage changes in Illinois using the Gravity Recovery and Climate Experiment (GRACE)," *Water Resour. Res.*, vol. 42, no. 12, pp. 1–7, 2006, doi: 10.1029/2006WR005374.
60. B. R. Scanlon, L. Longuevergne, and D. Long, "Ground referencing GRACE satellite estimates of groundwater storage changes in the California Central Valley, USA," *Water Resour. Res.*, vol. 48, no. 4, 2012, doi: https://doi.org/10.1029/2011WR011312.
61. M. Rodell, I. Velicogna, and J. S. Famiglietti, "Satellite-Based Estimates of Groundwater Depletion in India," *Nature*, vol. 460, no. 7258, pp. 999–1002, 2009, doi: 10.1038/nature08238.
62. P. Döll et al., "Impact of water withdrawals from groundwater and surface water on continental water storage variations," *J. Geodyn.*, vol. 59–60, pp. 143–156, 2012, doi: https://doi.org/10.1016/j.jog.2011.05.001.